Society for Immunotherapy of Cancer
sitc2024
NOV. 6-10 | HOUSTON

Poster 113

Label-free dynamic optical coherence microscopy assesses cytotoxicity in response to immune checkpoint inhibitors in ex vivo live tumor tissue

Chao J. Liu[1], Jewel Tulod[1], Yuan-I (Nina) Chen[1], Eric Wait[1], Christin Johnson[1], Ellen Wargowski[1], Todd Bakken[1], Sean Caenepeel[1], Pierre Cunin[1], Andrew Durette[1], Evan Flietner[1], Michael Korrer[1], Jonathan N Ouellette[1],Christina Scribano[1], Max Schiller[1], Lindsey Vedder[1], Kevin Eliceiri[2] and Michael Szulczewski[1]

[1]Elephas Biosciences, Madison, WI, [2]University of Wisconsin-Madison, Madison, WI.

elephas™

Introduction

- Cancer imaging assays typically use external labels, such as dyes, to assess treatment induced cytotoxicity
- Although dyes work well with tumor cell line monolayers and spheroids, they often fail to prove adequate for primary tumor tissues, where the native tumor microenvironment and architecture are maintained
- Dynamic optical coherence microscopy (dOCM), an emerging noninvasive, label-free imaging modality, analyzes temporal signals for fluctuations due to metabolic processes and cellular motions
- dOCM allows for longitudinal and nondestructive assessment of cell viability deep in intact tissue, removing the need for dyes
- Here we use dOCM to detect cytotoxic changes in tumor tissue in response to immune checkpoint inhibitor (ICI) treatment, and assess its alignment with the ground truth dye propidium iodide (PI)

Methods

Sample preparation: CT26 tumors were cut into fragments using an automated cutting instrument (Elephas). The tissue fragments were embedded in Matrigel (Corning) in polytetrafluoroethylene standing well inserts (Millipore Sigma) which were positioned in multi-well glass bottom plates (Ibidi).

Imaging: A customized multimodal imaging system (Elephas) was used to obtain dOCM and multiphoton microscopy (MPM) imaging data with modalities coaligned through a 15x, 0.8 numerical aperture objective.

dOCM imaging of cytotoxicity: Images were acquired using Elephas custom acquisition software. Time resolved, volumetric dOCM data were obtained to extract structural and viability data. To observe ICI-mediated cytotoxicity, fragments were imaged every 12 hours, except for during the addition of treatment. Baseline data were collected during the first 12 hours (-24 to -12 hours) of the experiment. Treatments (IgG, αPD-1, αPD-1 + αLAG3) were added at the 0 hour time point.

MPM imaging of cytotoxicity: A titanium-sapphire laser (Coherent) was tuned to 740 nm to excite nicotinamide adenine dinucleotide (phosphate) (NAD(P)H) and PI (1 μg/mL, Invitrogen). PI was added to the culture media 4 hours prior to imaging. The fragments were imaged at 0, 24 and 48 hours after treatment.

In vivo tumor growth inhibition: BALB/c mice implanted with CT26 tumors were treated with PBS (vehicle control) or 100 μg αPD-1 or αPD-1 + αLAG3 (N=30 per group) starting five days post implantation and continuing twice every week until tumors in the control group reached 2000 mm³.

Immunohistochemistry: Immunohistochemistry was performed on representative CT26 tumors from each of the treatment groups harvested 26 days after implant. Tumors were formalin-fixed, paraffin-embedded (FFPE), sectioned and stained with CD8, cleaved caspase 3 (CC3) and Ki67 antibodies.

Immunofluorescence: Multiplex immunofluorescence was performed on representative CT26 tumors from each of the treatment groups at the end of experimentation. Tumors were formalin-fixed, paraffin-embedded (FFPE), sectioned and stained with CD8 and CD4 antibodies, and DAPI.

Ex vivo cytokine analysis: Untreated, subcutaneous CT26 tumors were harvested at 200-300 mm³. Core needle biopsies (CNBs) were collected from excised tumors and cut into 300 μm thick slices. Slices were treated with IgG, αPD-1 or αPD-1 + αLAG3 antibodies for 20 hours. Conditioned media was collected for IFNγ analysis by ELISA after 20 hours of treatment.

1 dOCM detects chemically-induced cytotoxicity in syngeneic tumor tissue

Use of dOCM to assess cell viability in CT26 tumor fragments

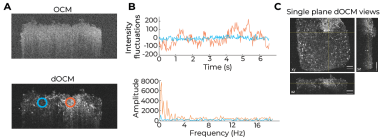

Accuracy of dOCM in assessing H_2O_2-induced cytotoxicity in CT26 tumor fragments using PI staining as ground truth

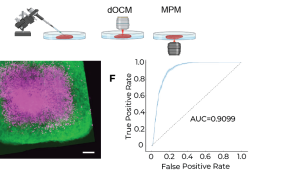

Cell viability imaging protocol using dOCM. (A) OCM and dOCM images of the same cross-section from a CT26 tumor fragment. Orange and blue circles represent live and dead regions of interest respectively. (B) Intensity profiles showing intensity fluctuations from the mean ($I(t) - \langle I(t) \rangle_t$, $I(t)$ = temporal intensity over time; top) and power spectral functions (bottom). Live frequency is defined as 0.1 Hz – 1 Hz. (C) Single plane views of a CT26 tumor fragment. Yellow lines indicate the positions of adjacent xz and yz images. The upper right corner of the fragment contains numerous live cells, whereas the rest of the tissue contains scattered live cells. Scale bars = 100 μm. (D) Multimodal imaging protocol. Local death in the center of CT26 fragments is introduced by microinjection of 3% H_2O_2. Volumetric data of the fragment is collected by dOCM first and then by MPM after the fragment is flipped. (E) Registered PI (magenta) and dOCM (green) images of the same fragment. The images show the average intensity projection of 100 μm over depth. Scale bar = 100 μm. (F) Receiver Operating Characteristic (ROC) curve of dOCM contrast for live/dead status when PI is used as ground truth.

2 dOCM detects heat-shock-induced cytotoxicity in primary human bladder tumor tissue

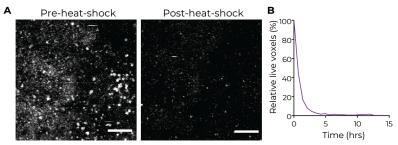

dOCM imaging of a 300 μM thick primary human bladder tumor fragment heat-shock-treated for 12 hours. (A) Images were collected prior to treatment (left) and after 10 hours of treatment (right). Scale bar = 100 μm. A qualitative reduction in dOCM contrast can be seen following treatment which is represented quantitatively in (B) as a change in the percentage of live voxels (live voxels/structural voxels) over time relative to time point 0 hrs. A timelapse video of this experiment and a supplemental experiment performed in primary human lung tumor tissue may be viewed by scanning the QR code on the bottom right hand corner of this poster.

3 dOCM detects ICI-mediated cytotoxicity in CT26 tumor fragments ex vivo

Experimental protocol

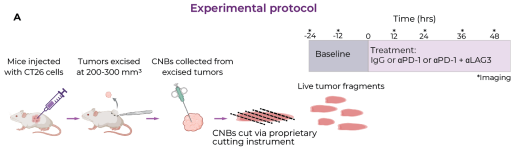

Time course of ICI-mediated cytotoxicity imaged using dOCM

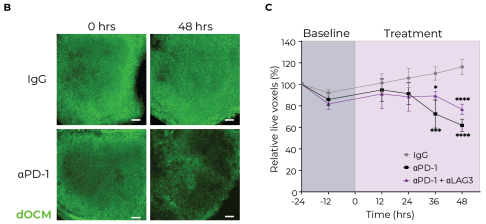

T-cells remain within fragments and IFNγ is increased with ICI treatment ex vivo

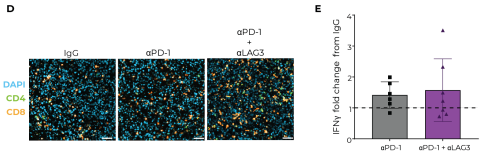

Time course dOCM imaging analysis of CT26 tumor fragments treated with immune checkpoint inhibitors. (A) Schematic showing experimental protocol of tumor processing, treatment and imaging. (B) Representative dOCM images of CT26 tumor fragments prior to treatment and following 48 hours of treatment with αPD-1 or IgG. Reduced dOCM contrast can be seen in the αPD-1-treated fragment at 48 hrs after treatment. Scale bar = 100 μm. (C) Time course dOCM imaging analysis of CT26 tumor fragments treated with IgG, αPD-1 or αPD-1 + αLAG3. (N = 4 tumors with a range of 3-12 fragments per time point and treatment. Relative live voxels (%) was calculated by dividing the number of live voxels by the total number of structural voxels over time relative to time point -24 hrs. A two-way ANOVA revealed a significant interaction between day and treatment ($F(10,119) = 3.430$, $P = 0.0006$). Tukey's multiple comparisons analysis showed a significant difference in the αPD-1 treated group between -24 hrs and 48 hrs ($P=0.009$). Error bars represent SEM. *$P<0.05$, **$P<0.001$, ****$P<0.0001$. (D) Representative multiplex immunofluorescence images for CD8 (orange) and CD4 (green) staining show T-cells are maintained in fragments from all treatment groups. Scale bar = 50 μm. (E) Graph showing the fold change from IgG in IFNγ cytokine concentrations for αPD-1 (50 μg/μL) or αPD-1 (50 μg/μL) + αLAG3 (50 μg/μL) following 20 hrs of treatment. N = 6 and 7 tumors for αPD-1 and αPD-1 + αLAG3 groups, respectively. Error bars represent SEM.

4 ICI-mediated CT26 tumor growth inhibition in vivo aligns with dOCM observations ex vivo

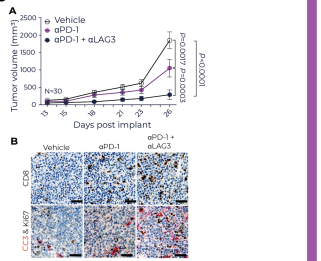

(A) In vivo CT26 tumor growth curves from mice treated with vehicle, αPD-1, or αPD-1+αLAG3 (n = 30 per group). Error bars represent SEM. Significant tumor growth inhibition was observed with αPD-1 alone or the combination of αPD-1 + αLAG3. (B) Immunohistochemistry conducted on tumors harvested 26 days after implant showing qualitative increases in CD8 and CC3 staining following treatment with αPD-1 or αPD-1 + αLAG3. Scale bar = 50 μm.

5 MPM imaging of PI detects ICI-mediated cytotoxicity in CT26 tumor fragments ex vivo

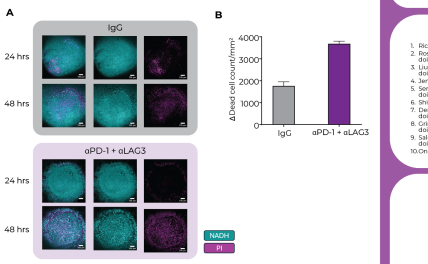

(A) Representative MPM images showing IgG- or αPD-1 + αLAG3-treated tumor fragments at 24 hrs of treatment compared to 48 hrs of treatment. (B) Bar graphs report the difference in dead cell count/mm² at 48 hours of treatment versus 24 hours of treatment. The difference in dead cell count/mm² was calculated by dividing the number of PI-positive cells by the NAD(P)H total area. n = 6 fragments per group across 2 tumors with 4 z-planes imaged per fragment. Error bars represent SEM.

Conclusions

- dOCM, a non-destructive, label-free imaging technique, can be used to measure ICI-mediated cytotoxicity in tumor tissue
- Ex vivo assessment of ICI-mediated cytotoxicity with dOCM reveals efficacy that is aligned with in vivo tumor growth inhibition in the murine syngeneic tumor model CT26
- dOCM and the ground truth dye propidium iodide correspond in their assessment of ICI-mediated cytotoxicity ex vivo
- These data support the use of dOCM to assess the efficacy of immunotherapy in tumor tissue ex vivo

Acknowledgments

Human tissue samples were provided by the Cooperative Human Tissue Network which is funded by the National Cancer Institute.

The authors thank the following individuals for their contributions to this work; John R Rafter, Nicholas Kaplewski and Katherine Rexroad for their advice in the development of this poster.

Some figures created in BioRender.com.

References

1. Ricciardi C, Nicoletti I. *Nat Protoc.* 2006;1(3):1458-1461. doi:10.1038/nprot.2006.238
2. Rosenberg M, Azevedo NF, Ivask A. *Sci Rep.* 2019;9(1):6483. Published 2019 Apr 24. doi:10.1038/s41598-019-42906-3
3. Liu CJ, Smith JT, Wang Y, et al. *Biomed Opt Express.* 2024;15(3):1408-1417. Published 2024 Feb 5. doi:10.1364/BOE.509835
4. Jenkins RW, Aref AR, Lizotte PH, et al. *Cancer Discov.* 2018;8(2):196-215. doi:10.1158/2159-8290.CD-17-0833
5. Sengal AT, Bonazzi V, Smith D, et al. *NPJ Precis Oncol.* 2023;7(1):127. Published 2023 Dec 6. doi:10.1038/s41698-023-00478-6
6. Shimokawa M, Yoshizumi T, Itoh S, et al. *Cancer Sci.* 2020;111(4):1228-1240. doi:10.1111/cas.14320
7. Demyanyk R, Efimova I, Lin A, Declerck H, Kryske DV. *Cells.* 2020;9(3):703. Published 2020 Mar 13. doi:10.3390/cells9030703
8. Grimm FA, Iwata Y, Sirenko O, Bittner M, Rusyn I. *Assay Drug Dev Technol.* 2015;13(9):529-546. doi:10.1089/adt.2015.659
9. Salehi F, Behboudi H, Kavosi G, Ardestani SK. *Sci Rep.* 2017;7(1):2553. Published 2017 May 31. doi:10.1038/s41598-017-02633-z
10. Omer E, Gray SG, Finn SP. *Methods Mol Biol.* 2023;2645:263-275. doi:10.1007/978-1-0716-3056-3_17

Scan here for more information